Gert Strobl

The Physics of Polymers

Concepts for Understanding Their Structures and Behavior

Third Revised and Expanded Edition
With 295 Figures and 2 Tables

Springer

Gert Strobl

The Physics of Polymers

Concepts for Understanding Their Structures and Behavior

Third Revised and Expanded Edition
With 295 Figures and 2 Tables

Springer

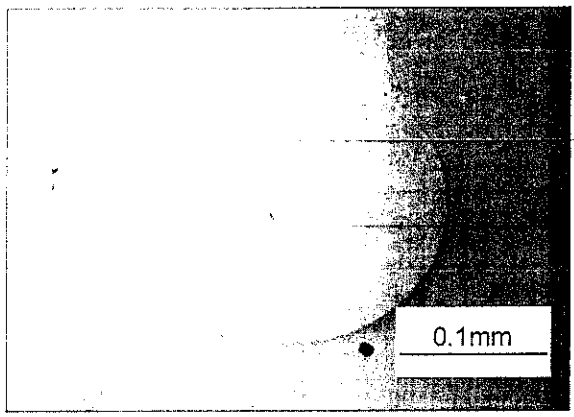

Fig. 4.26. Macroscopic domains in a two-phase PS/PBr$_x$S-(1:1) mixture, formed after 2 h of annealing [21]

The curves in Fig. 4.25 are in agreement with this law, which can therefore be employed for a determination of O_{12}. The time dependence of O_{12} is given in the lower half of Fig. 4.25. Results indicate a decrease of O_{12} inverse to t,

$$O_{12} \propto t^{-1} \,. \tag{4.121}$$

Here, we cannot discuss the theories developed for the late stage kinetics, but the physical background must be mentioned, since it is basically different from the initial stages discussed above. Whereas the kinetics in the initial stages is based on diffusive processes only, the late stages are controlled by convective flow. The driving force originates from the excess free energy of the interfaces. The natural tendency is a reduction of O_{12} and this is achieved by a merging of smaller domains into larger ones.

The latter mechanism remains effective up to the end; however, the structure characteristics must finally change as the similarity property cannot be maintained. The very end is a macroscopic phase separation, as shown, for example, in Fig. 4.26 and clearly, the final structure is always of the same type independent of whether phase separation has started by spinodal decomposition or by nucleation and growth.

4.4 Block Copolymer Phases

If two different polymeric species are coupled together by chemical links, one obtains block copolymers. These materials possess peculiar properties and we will consider them in this section.

In the discussion of the behavior of binary polymer mixtures, we learned that, in the majority of cases, they separate into two phases. As the linkages in block copolymers inhibit such a macroscopic phase separation, one may

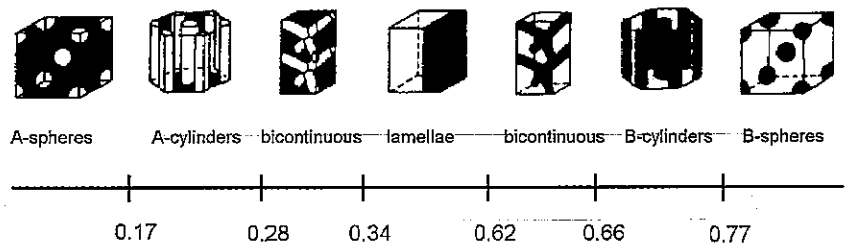

Fig. 4.27. Different classes of microphase separated structures in block copolymers, as exemplified by PS-*block*-PI. The *numbers* give the phase boundaries in terms of the volume fraction of the PS blocks. Figure taken from a review article by Bates and Frederickson [29]

wonder how these systems react under comparable conditions. Figure 4.27 gives the answer with a drawing: The A's and B's still segregate but the domains have only mesoscopic dimensions corresponding to the sizes of the single blocks. In addition, as all domains have a uniform size, they can be arranged in regular manner. As a result ordered mesoscopic lattices emerge. In the figure it is also indicated that this **microphase separation** leads to different classes of structures in dependence on the ratio between the degrees of polymerization of the A's and B's. For $N_A \ll N_B$ spherical inclusions of A in a B-matrix are formed and they set up a body-centered cubic lattice. For larger values N_A, but still $N_A < N_B$, the A-domains have a cylindrical shape and are arranged in a hexagonal lattice. Layered lattices form under essentially symmetrical conditions, i.e., $N_A \approx N_B$. Then, for $N_A > N_B$, the phases are inverted and the A-blocks now constitute the matrix.

In addition to these lattices composed of spheres, cylinders and layers, periodic structures occur under special conditions where both phases are continuous and interpenetrate each other. These bicontinuous **gyroid** structures exist only in a narrow range of values N_A/N_B, between the regimes of the cylindrical and lamellar structures and, as it appears, only when the repulsion forces between the A's and the B's are not too strong. To be sure, the figure depicts the structures observed for polystyrene-*block*-polyisoprene, but these are quite typical. Spherical, cylindrical and layer-like domains are generally observed in all block copolymers. Less is known about how general the bicontinuous special types like the gyroid lattices are.

The majority of synthesized compounds are **di-block copolymers** composed of one A-chain and one B-chain; however, tri-blocks and multiblocks, comprising an arbitrary number of A-chains and B-chains, can be prepared as well. One can also proceed one step further and build up multiblocks that incorporate more than two species, thus again increasing the variability. The question may arise as to whether all these modifications result in novel structures. In fact, this is not the case. The findings give the impression that at least all block copolymers composed of two species exhibit qualitatively sim-

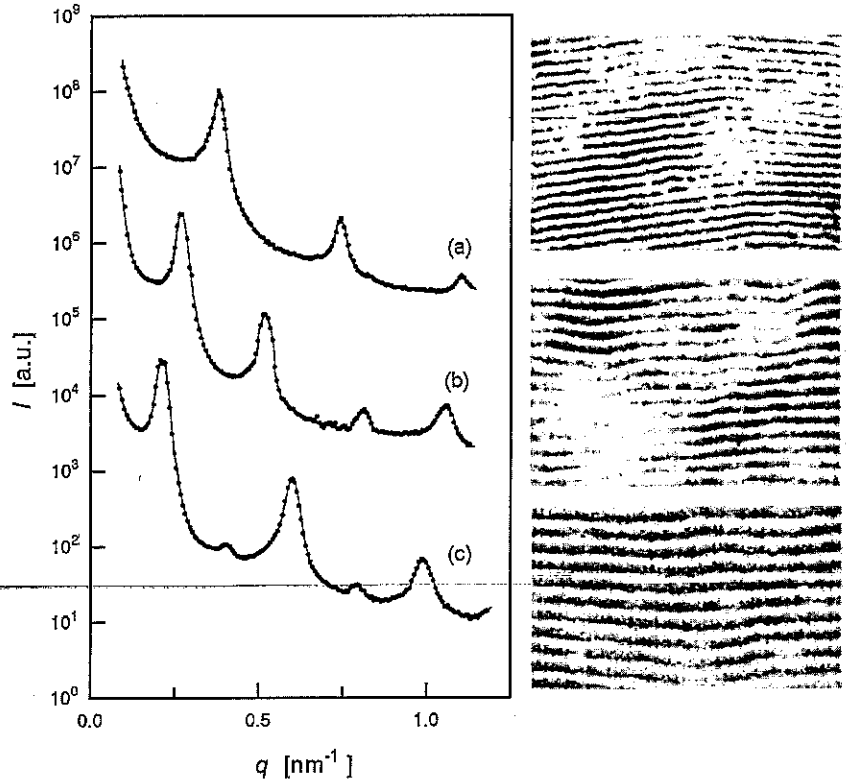

Fig. 4.28. SAXS curves measured for a series of PS-*block*-PI with different molar masses in the microphase separated state: (a) $M = 2.1 \times 10^4\,\mathrm{g\,mol^{-1}}$, $\phi(\mathrm{PS}) = 0.53$; (b) $M = 3.1 \times 10^4\,\mathrm{g\,mol^{-1}}$, $\phi(\mathrm{PS}) = 0.40$; (c) $M = 4.9 \times 10^4\,\mathrm{g\,mol^{-1}}$, $\phi(\mathrm{PS}) = 0.45$ (*left*). Transmission electron micrographs obtained using ultra-thin sections of specimen stained with OsO_4 (*right*). Structures belong to the layer regime. Data from Hashimoto et al. [30]

ilar phase behaviors. Changes then occur for ternary systems. For the latter, the observed structures still possess periodic orders, but the lattices are more complex. Here, we shall only be concerned with the simplest systems, the di-block copolymers.

Suitable methods for an analysis of block copolymer structures are electron microscopy and small angle X-ray scattering (SAXS) experiments. Figure 4.28 gives an example and on the left-hand side presents scattering curves obtained for a series of polystyrene-*block*-polyisoprenes where both blocks had similar molar mass. Structures belong to the layer regime and one correspondingly observes series of equidistant Bragg reflections. The right-hand side depicts micrographs obtained for the same samples in an electron microscope using

ultra-thin sections of specimens where the polyisoprene blocks were stained with OsO_4. The layered structure is clearly visible and one notices an increase of the layer thicknesses with the molar masses of the blocks.

In binary polymer mixtures, under favorable conditions one finds homogeneous phases. They either arise if the forces between unlike monomers are attractive or, generally, if the molar masses are sufficiently low. Block copolymers behave similarly and can also have a homogeneous phase. It actually has a larger stability range than the corresponding binary mixture. Recall that for a symmetric mixture ($N_A = N_B$) the two-phase region begins at (Eq. (4.35))

$$(\chi N_A)_c = 2 \, .$$

If a symmetric di-block copolymer is formed from the same A- and B-chains, the transition between the homogeneous phase and the microphase separated state takes place at a higher χ, namely for

$$(\chi N_A)_c \approx 5 \, . \tag{4.122}$$

The complete phase diagram of a block copolymer is displayed in Fig. 4.29 in a schematic representation. Variables are the volume fraction of the A-blocks

$$\phi_A = \frac{N_A}{N_A + N_B} \tag{4.123}$$

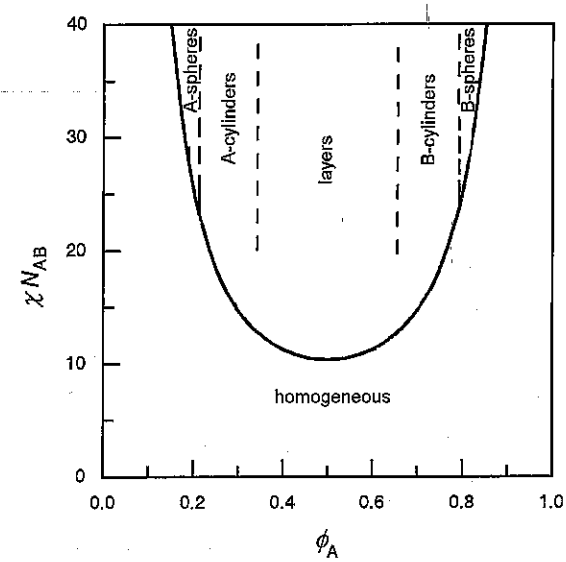

Fig. 4.29. Phase diagram of a di-block copolymer in a schematic representation. The curve describes the points of transition between the homogeneous phase and the microphase separated states. The ordered states are split into different classes as indicated by the *dashed boundary lines*. They are only shown here for the region of higher values of χN_{AB} away from the phase transition line

and the product χN_{AB}, where N_{AB} describes the total degree of polymerization

$$N_{AB} = N_A + N_B \, .$$

The transition line separating the homogeneous phase from the various microphase separated structures has an appearance similar to the binodal of a polymer mixture. There is, however, a basic difference: In the block copolymer case, we are dealing with a one component system rather than a binary mixture. The line therefore relates to a phase transition rather than to a miscibility gap. It should also be noted that, in contrast to the binodal of a mixture, the transition line tells us nothing about the internal composition of the microphases. In principle, these could be mixed states; however, with the exception of situations near the transition line, compositions are mostly close to pure A- or B-states. The schematic drawing indicates only the structures arising under the conditions of a **strong segregation**, $\chi N_{AB} \gg 10$, where solely lattices of spheres, cylinders and layers are found. The situation for a **weak segregation** with χN_{AB} just above the critical value is more complicated. Here, also the bicontinuous structures are found and subtle features decide about their stability relative to the three major forms.

4.4.1 Layered Structures

Each of the ordered structures represents under the respective conditions the state with the lowest Gibbs free energy. Calculations of the Gibbs free energies and comparisons between the various lattices and the homogeneous phase can therefore provide an understanding of the phase diagram. In addition, they make it possible to determine the structure parameters.

Theoretical analyses were carried out by Meier and Helfand. A full presentation lies outside our possibilities but in order to gain at least an impression of the approaches, we will pick out the layered structures as an example and discuss the equilibrium conditions. The main result will be a power law that formulates the dependence of the layer thicknesses on the degree of polymerization of the blocks.

If we think about the structural changes that accompany a transition from the homogeneous phase to an ordered layer structure, we find three contributions to the change in the Gibbs free energy

$$\Delta g_p = \Delta h_p - T\Delta s_{p,if} - T\Delta s_{p,conf} \, . \qquad (4.124)$$

There is a change in enthalpy, a change in entropy following from the arrangement of the junction points along the interfaces and another change in entropy resulting from altered chain conformations. We write the equation in terms of quantities referring to one di-block polymer.

The driving force for the transitions comes from the enthalpic part. In the usual case of unfavorable AB-interactions, i.e., $\chi > 0$, there is a gain

in enthalpy on unmixing. We assume a maximum gain, achieved when we have a random distribution of the monomers in the homogeneous phase and a perfect segregation in the lamellar phase. Then the enthalpy change per polymer, Δh_p, is given by

$$\Delta h_\mathrm{p} = -kT\chi N_\mathrm{AB}\phi_\mathrm{A}(1-\phi_\mathrm{A}) + \Delta h_\mathrm{p,if} \,. \tag{4.125}$$

The first term follows directly from Eq. (4.24). The second term, $\Delta h_\mathrm{p,if}$, accounts for an excess enthalpy that is contributed by the interfaces. To see the background, bear in mind that interfaces always possess a finite thickness, typically in the order of one to several nm. Within this transition layer the A's and B's remain mixed, which leads to an increase in enthalpy proportional to χ and to the number of structure units in the transition layer. Let the thickness of the transition layer be d_t and the interface area per polymer o_p, then we may write

$$\Delta h_\mathrm{p,if} \simeq kT\chi\frac{o_\mathrm{p}d_\mathrm{t}}{v_\mathrm{c}} \,. \tag{4.126}$$

v_c again is the volume of the structure unit, commonly chosen for both the A- and B-chains.

The two entropic parts both work in the opposite direction. There is first the loss in entropy, which results from the confinement of the junction points, being localized in the transition layer. For a layered phase with layer thicknesses d_A and d_B, and therefore a period

$$d_\mathrm{AB} = d_\mathrm{A} + d_\mathrm{B} \,, \tag{4.127}$$

$\Delta s_\mathrm{p,if}$ may be estimated using a standard equation of statistical thermodynamics

$$\Delta s_\mathrm{p,if} \simeq k\ln\frac{d_\mathrm{t}}{d_\mathrm{A}+d_\mathrm{B}} \,. \tag{4.128}$$

The second entropic contribution, $\Delta s_\mathrm{p,conf}$, accounts for a decrease in entropy, which follows from a change in the chain conformations. The Gaussian conformational distribution found in the homogeneous phase cannot be maintained in the microphase separated state. Formation of a layer structure leads, for steric reasons, necessarily to a chain stretching, which in turn results in a loss in entropy. For a qualitative description we employ the previous Eq. (2.93),

$$\Delta s_\mathrm{p,conf} \simeq -k\left(\frac{R}{R_0}\right)^2 \,, \tag{4.129}$$

where R and R_0 are now the end-to-end distances of the block copolymer in the layered and the homogeneous phase, respectively. Assuming that chain sizes and layer spacings are linearly related, by

$$R = \beta d_\mathrm{AB} \,, \tag{4.130}$$

the equation converts into

$$\Delta s_{\mathrm{p,conf}} \simeq -k\beta^2 \left(\frac{d_{\mathrm{AB}}}{R_0}\right)^2 . \tag{4.131}$$

We can now search for the equilibrium. First note that o_{p} and d_{AB} are related by the obvious equation

$$o_{\mathrm{p}} d_{\mathrm{AB}} = N_{\mathrm{AB}} v_{\mathrm{c}} . \tag{4.132}$$

We therefore have only one independent variable, for example o_{p}. Using all the above expressions, we obtain for the change in the Gibbs free enthalpy

$$\frac{1}{kT}\Delta g_{\mathrm{p}} = -\chi N_{\mathrm{AB}} \phi_{\mathrm{A}} (1-\phi_{\mathrm{A}}) + \chi o_{\mathrm{p}} d_{\mathrm{t}} v_{\mathrm{c}}^{-1} + \ln \frac{d_{\mathrm{t}}}{d_{\mathrm{AB}}} + \beta^2 \left(\frac{d_{\mathrm{AB}}}{R_0}\right)^2 . \tag{4.133}$$

If we neglect the slowly varying logarithmic term, we obtain for the derivative

$$\frac{1}{kT}\frac{\mathrm{d}\Delta g_{\mathrm{p}}}{\mathrm{d}o_{\mathrm{p}}} = \chi \frac{d_{\mathrm{t}}}{v_{\mathrm{c}}} - 2\beta^2 \frac{N_{\mathrm{AB}}^2 v_{\mathrm{c}}^2}{R_0^2} \frac{1}{o_{\mathrm{p}}^3} . \tag{4.134}$$

The equilibrium value of o_{p} follows as

$$o_{\mathrm{p}}^3 \propto 2\frac{v_{\mathrm{c}}^3}{R_0^2 d_{\mathrm{t}} \chi} N_{\mathrm{AB}}^2 . \tag{4.135}$$

With

$$R_0^2 \propto v_{\mathrm{c}}^{2/3} N_{\mathrm{AB}} \tag{4.136}$$

we find

$$o_{\mathrm{p}}^3 \propto \frac{v_{\mathrm{c}}^{7/3}}{d_{\mathrm{t}} \chi} N_{\mathrm{AB}} . \tag{4.137}$$

Replacement of o_{p} by d_{AB} gives us the searched-for result

$$d_{\mathrm{AB}}^3 = \frac{N_{\mathrm{AB}}^3 v_{\mathrm{c}}^3}{o_{\mathrm{p}}^3} \propto \chi d_{\mathrm{t}} v_{\mathrm{c}}^{2/3} N_{\mathrm{AB}}^2 . \tag{4.138}$$

How does this result compare with experiments? Figure 4.30 depicts the data obtained for the samples of Fig. 4.28. Indeed, the agreement is perfect. The slope of the line in the double logarithmic plot exactly equals the predicted exponent 2/3.

4.4.2 Pretransitional Phenomena

A characteristic property of polymer mixtures in the homogeneous phase is the increase of the concentration fluctuations associated with an approaching of the point of unmixing. A similar behavior is found for the homogeneous phase of block copolymers and a first example is given in Fig. 4.31. The figure

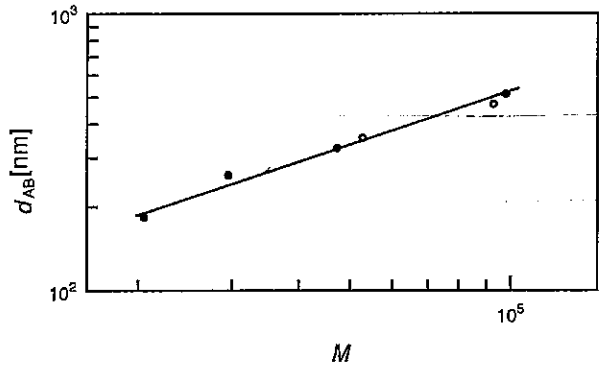

Fig. 4.30. Set of samples of Fig. 4.28. Molecular weight dependence of the layer spacing d_{AB}

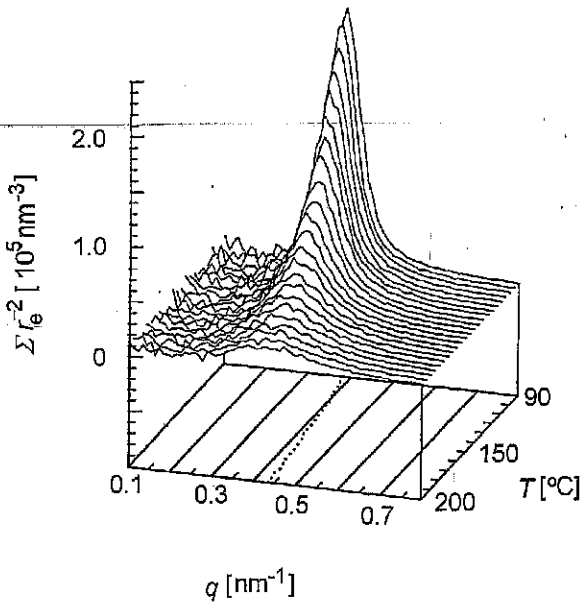

Fig. 4.31. SAXS curves measured for a polystyrene-*block*-polyisoprene ($M = 1.64 \times 10^4$ g mol^{-1}, ϕ(PS) = 0.22) in the homogeneous phase. The *dotted line* on the base indicates the temperature dependence of the peak position [31]

shows scattering functions measured for a PS-*block*-PI under variation of the temperature. The temperature of the transition to the microphase separated state is located around 85 °C, just outside the temperature range of the plot. The curves exhibit a peak, with an intensity that strongly increases when the temperature moves towards the transition point.

The feature in common with the polymer mixtures is the intensity increase; however, we can also see a characteristic difference: The maximum of

the scattering intensity and the largest increase are now found for a finite scattering vector $q_{\max}$, rather than at $q = 0$. As scattering curves display the squared amplitudes of wave-like concentration fluctuations, the observation tells us that concentration fluctuations with wavevectors in the range $|\boldsymbol{k}| \approx q_{\max}$ are always large compared to all the others and show a particularly strong increase on approaching the phase transition. What do these observations mean? Clearly, they remind us of the pretransitional phenomena observed for second order phase transitions. There, the approach of the transition point is always associated with an unusual increase of certain fluctuations. Hence as it appears, one also finds properties in the homogeneous phase that have much in common with the behavior of critical systems, not only for polymer mixtures, but also for block copolymers.

The general shape of the scattering curve, showing a maximum at some $q_{\max}$ and going to zero for $q \to 0$ is conceivable. As explained in Sect. A.3.2 of the Appendix, the forward scattering, $S(q \to 0)$, always relates to the fluctuation of the number of particles in a fixed macroscopic volume. In our case, this refers to both the A's and the B's. The strict coupling between A- and B-chains in the block copolymers completely suppresses number fluctuations on length scales that are large compared to the size of the block copolymer. The limiting behavior of the scattering function, $S(q \to 0) \to 0$, reflects just this fact. On the other hand, for large q's, scattering of a block copolymer and of the corresponding polymer mixture composed of the decoupled blocks, must be identical because here only the internal correlations within the A- and B-chains are of importance. As a consequence, asymptotically the scattering law of ideal chains, $S(q) \propto 1/q^2$, shows up again. Hence, one expects an increase in the scattering intensity coming down from large q's and when emanating from $q = 0$ as well. Both increases together produce a peak, located at a certain finite $q_{\max}$.

The increase of the intensity with decreasing temperature reflects a growing tendency for associations of the junction points accompanied by some short-ranged segregation. As long as this tendency is not too strong, this could possibly occur without affecting the chain conformations, i.e., chains could still maintain Gaussian properties. If one adopts this view, then the scattering function can be calculated explicitly. Leibler and others derived the following expression for the scattering function per structure unit S_c:

$$\frac{1}{S_c(q)} = \frac{1}{S_c^0(q)} - 2\chi \tag{4.139}$$

with $S_c^0(q)$, the scattering function in the athermal case, given by

$$\begin{aligned} S_c^0(q) N_{AB} S_D\left(R_0^2 q^2\right) = {} & \phi(1-\phi) N_A N_B S_D\left(R_A^2 q^2\right) S_D\left(R_B^2 q^2\right) \\ & - \frac{1}{4}\left[N_{AB} S_D\left(R_0^2 q^2\right) - \phi N_A S_D\left(R_A^2 q^2\right)\right. \\ & \left. - (1-\phi) N_B S_D\left(R_B^2 q^2\right)\right]^2 . \end{aligned} \tag{4.140}$$

R_0^2 denotes the mean squared end-to-end distance of the block copolymer, given by

$$R_0^2 = R_A^2 + R_B^2 \,. \tag{4.141}$$

With regard to the effect of χ, Eq. (4.139) is equivalent to Eq. (4.91). Indeed, the physical background of both equations is similar and they are obtained in an equal manner by an application of the random phase approximation (RPA). The interested reader can find the derivation in Sect. A.4.1 in the Appendix.

Importantly, Eq. (4.139) describes the effect of χ directly. It becomes very clear if one plots the inverse scattering function. Then changes in χ result in parallel shifts of the curves only. Figure 4.32 depicts the results of model calculations for a block copolymer with a volume fraction of polystyrene blocks of $\phi = 0.22$, in correspondence to the sample of Fig. 4.31. The curves were obtained for the indicated values of the product χN_{AB}.

Obviously the calculations represent the main features correctly: They yield a peak at a certain q_{max}, which grows in intensity with increasing χ, i.e., with decreasing temperature. The important result comes up for $\chi N_{AB} = 21.4$. For this value we find a diverging intensity at the position of the peak, $S(q_{max}) \to \infty$. This is exactly the signature of a critical point. We thus realize that the RPA equation formulates a critical transition with a continuous passage from the homogeneous to the ordered phase. When dealing with critical phenomena, it is always important to see the order parameter. Here it is

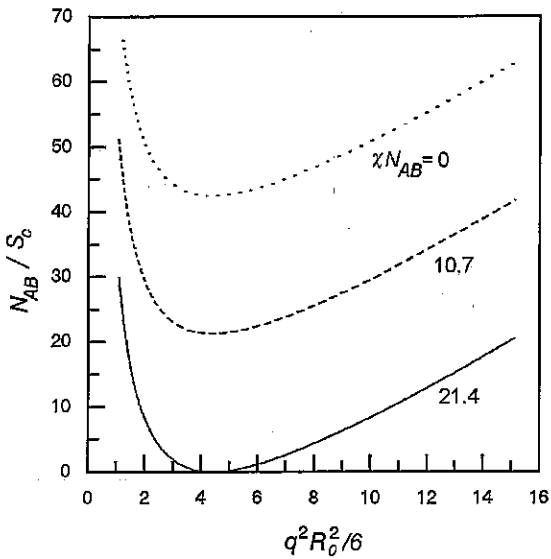

Fig. 4.32. Theoretical scattering functions of a block copolymer with $\phi = 0.22$, calculated for the indicated values of χN_{AB}

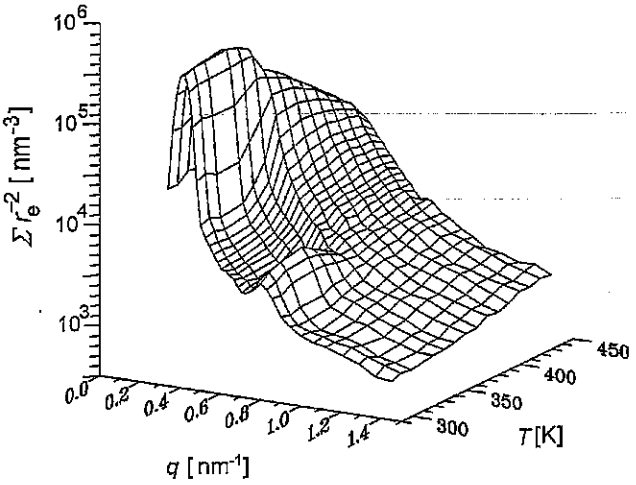

Fig. 4.33. SAXS curves measured for a PS-*block*-PI (ϕ(PS) = 0.44, $M = 1.64 \times 10^4$ g mol^{-1}) in the temperature range of the microphase separation. The transition occurs at $T_t = 362$ K. Data from Stühn et al. [32]

of a peculiar nature. According to the observations it is associated with the amplitudes of the concentration waves with $|\boldsymbol{k}| = q_{\max}$.

For $\phi = 0.22$, the critical point is reached for $N_{\mathrm{AB}}\chi = 21.4$. With the aid of the RPA result, Eq. (4.140), one can calculate the critical values for all ϕ's. In particular, for a symmetric block copolymer one obtains

$$\chi N_{\mathrm{AB}} = 10.4\,.$$

This is the lowest possible value and the one mentioned in Eq. (4.122).

In polymer mixtures, one calls the curve of points in the phase diagram, where $S(q = 0)$ apparently diverges, the spinodal. One can use the same notion for block copolymers and determine this curve in an equal manner by a linear extrapolation of scattering data measured in the homogeneous phase. We again denote this spinodal by $T_{\mathrm{sp}}(\phi)$.

Regarding all these findings, one could speculate that the microphase separation might take place as a critical phase transition in the strict sense, at least for block copolymers with the critical composition associated with the lowest transition temperature. In fact, experiments that pass over the phase transition show that this is not true and they also point to other limitations of the RPA treatment. Figure 4.33 presents scattering curves obtained for a polystyrene-*block*-polyisoprene near to the critical composition (ϕ(PS) = 0.44) in a temperature run through the transition point. As we can see, the transition is not continuous up to the end but is associated with the sudden appearance of two Bragg reflections. Hence, although the global behavior is dominated by the steady growth of the concentration fluctuations

typical for a critical behavior, finally there is a discontinuous step, which converts this transition into one of **weakly first order**.

There exists another weak point in the RPA equation. As a basic assumption, it implies that chains in the homogeneous phase maintain Gaussian statistical properties up to the transition point. The reality is different and this is not at all surprising: An increasing tendency for an association of the junction points also necessarily induces a stretching of chains, for the same steric reasons that in the microphase separated state lead to the specific power law Eq. (4.138). This tendency is shown by the data presented in Fig. 4.33 and, even more clearly, by the results depicted in Fig. 4.31. In both cases, $q_{\max}$ shifts to smaller values with decreasing temperature, as is indicative for chain stretching.

The details of the transition are interesting. Figure 4.34 depicts the temperature dependence of the inverse peak intensity $I^{-1}\,(q_{\max})$.

Equation (4.139) predicts a dependence

$$S(q_{\max})^{-1} \propto \chi_{\mathrm{sp}} - \chi\,, \tag{4.142}$$

or, assuming a purely enthalpic χ with $\chi \propto 1/T$ (Eq. (4.22)),

$$S(q_{\max})^{-1} \propto T_{\mathrm{sp}}^{-1} - T^{-1}\,. \tag{4.143}$$

The findings, however, are different. We can see that the data follow a linear law only for temperatures further away from the transition point and then

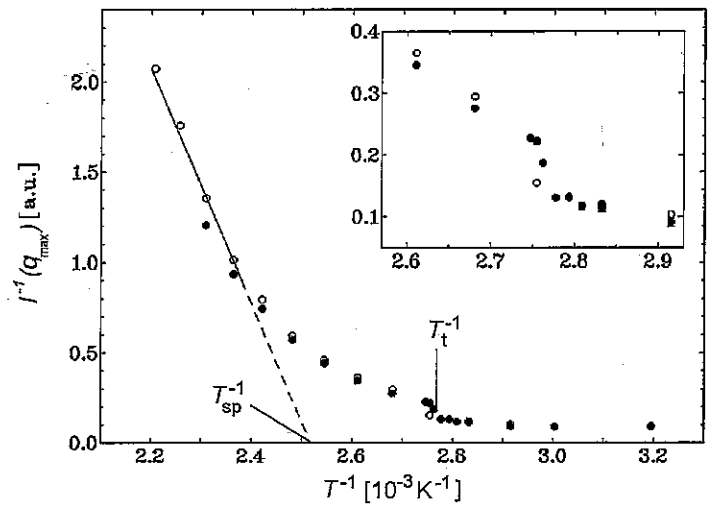

Fig. 4.34. Measurements shown in Fig. 4.33: Temperature dependence of the reciprocal peak intensity, showing deviations from the RPA predictions. The linear extrapolation determines the spinodal temperature

deviate towards higher values. The transition is retarded and does not take place until a temperature 35 K below the spinodal point is reached. According to theoretical explanations, which we cannot further elaborate on here, the phenomenon is due to a lowering of the Gibbs free energy, caused by the temporary short-range order associated with the fluctuations. The short-range order implies local segregations and thus a reduction of the number of AB-contacts, which in turn lowers the Gibbs free energy. We came across this effect earlier in the discussion of the causes of the energy lowering observed in computer simulations of low molar mass mixtures. Remember that there the effect exists only for low enough molar masses, since for high molar masses a short-range ordering becomes impossible. The same prerequisite holds for block copolymers and this is also formulated by the theories.

The short-range ordering is even more pronounced for asymmetric block-copolymers with $\phi_A \ll \phi_B$, which form in the microphase separated state

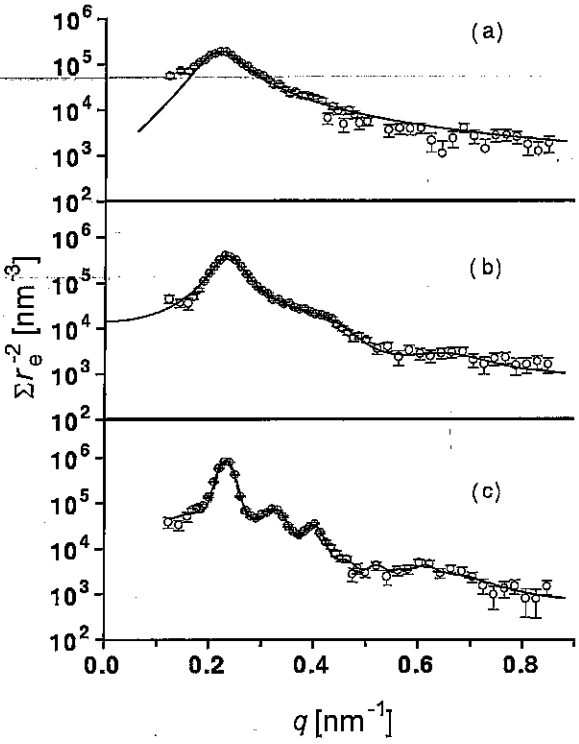

Fig. 4.35. PS-*block*-PI (ϕ(PS) = 0.11): (a) Scattering curves referring to the homogeneously disordered state (T = 458 K), (b) the state of liquid-like order between spherical domains (T = 413 K), and (c) the bcc ordered state (T = 318 K). The *continuous lines* are fits of structural models for the different states of order. From Schwab and Stühn [33]

a bcc-lattice of spheres. The fluctuation-affected temperature range between T_{sp} and T_t is even larger and the short-range ordering here shows up quite clearly in the scattering curves. Figure 4.35(b) presents as an example the scattering curve obtained for polystyrene-*block*-polyisoprene ($\phi(PS) = 0.11$) at $T = 413\,K$ ($T_{sp} = 450\,K$, $T_t = 393\,K$) in a comparison with scattering curves measured above T_{sp} in the homogeneous phase (a) and in the microphase separated state respectively (c). Curve (c) shows the Bragg reflections of a bcc-lattice and the data points in (a) are perfectly reproduced by the RPA equation. Interestingly, the data points in (b) are well-represented by a curve calculated for the scattering of hard spheres with liquid-like ordering; the continuous line drawn through the data points was obtained using the Perkus–Yevick theory, which deals with such liquids. Hence, the ordering during cooling of this block copolymer proceeds in two steps, beginning with the formation of spherical domains that are then placed at the positions of a lattice. The second step takes place when the repulsive interaction reaches a critical value.

Further Reading

K. Binder: *Spinodal Decomposition* in P. Haasen (Ed.): Material Science and Technology, Vol. 5 *Phase Transitions in Materials*, VCH Publishers, 1991

P.J. Flory: *Principles of Polymer Chemistry*, Cornell University Press, 1953

P.-G. de Gennes: *Scaling Concepts in Polymer Physics*, Cornell University Press, 1979

I. Goodman: Developments in Block Copolymers, Vol. 1, Applied Science Publishers, 1982

I. Goodman: Developments in Block Copolymers, Vol. 2, Applied Science Publishers, 1985

I. Hamley: *Block Copolymers*, Oxford University Press, 1999

T. Hashimoto: *Structure Formation in Polymer Systems by Spinodal Decomposition* in R.M. Ottenbrite, L.A. Utracki, S. Inoue (Eds.): Current Topics in Polymer Science, Vol. 2, Hanser, 1987

D.R. Paul, S. Newman (Eds.): *Polymer Blends, Vols. 1 and 2*, Academic Press, 1978

References

T. Hashimoto, J. Kumaki, and H. Kawai. *Macromolecules*, 16:641, 1983.

T. Koch and G.R. Strobl. *J. Polym. Sci., Polym. Phys. Ed.*, 28:343, 1990.

A. Sariban and K. Binder. *Macromolecules*, 21:711, 1988.

C.C. Han, B.J. Bauer, J.C. Clark, Y. Muroga, Y. Matsushita, M. Okada, T. Qui, T. Chang, and I.C. Sanchez. *Polymer*, 29:2002, 1988.

G.R. Strobl. *Macromolecules*, 18:558, 1985.

M. Takenaka and T. Hashimoto. *J. Chem. Phys.*, 96:6177, 1992.

F.S. Bates and G.H. Frederickson. *Ann. Rev. Phys. Chem.*, 41:525, 1990.

T. Hashimoto, M. Shibayama, and H. Kawai. *Macromolecules*, 13:1237, 1980.

A. Lehmann. *Diplomarbeit*, Physikalisches Institut, Universität Freiburg, 1989.

B. Stühn, R. Mutter, and T. Albrecht. *Europhys. Lett.*, 18:427, 1992.

M. Schwab and B. Stühn. *Phys. Rev. Lett.*, 76:924, 1996.

R. Eppe, E.W. Fischer, and H.A. Stuart. *J. Polym. Sci.*, 34:721, 1959.

B. Kanig. *Progr. Colloid Polym. Sci.*, 57:176, 1975.

A.S. Vaughan and D.C. Bassett. *Comprehensive Polymer Science, Vol.2*, page 415. Pergamon Press, 1989.

G.H. Michler. *Kunststoff-Mikromechanik*, page 187. Hanser, 1992.

S. Magonov and Y. Godovsky. *American Laboratory*, 31:52, 1999.

C.W. Bunn. *Trans. Farad. Soc.*, 35:482, 1939.

M. Kimmig, G. Strobl, and B. Stühn. *Macromolecules*, 27:2481, 1994.

T. Albrecht and G.R. Strobl. *Macromolecules*, 28:5827, 1995.

T. Albrecht. *Dissertation*, Universität Freiburg, 1994.

R. Mutter, W. Stille, and G. Strobl. *J. Polym. Sci.,Polym. Phys. Ed.*, 31:99, 1993.

C. Hertlein, K. Saalwaechter, and G. Strobl. *Polymer*, 47:7216, 2006.

G.S. Ross and L.J. Frolen. *Methods of Experimental Physics, Vol.16B*, page 363. Academic Press, 1980.

Y.G. Lei, C.M. Chan, J.X. Li, K.M. Ng, Y. Wang, Y. Jiang, and L. Lin. *Macromolecules*, 35:6751, 2002.

M. Massa and K. Dalnoki-Veress. *Phys. Rev. Lett.*, 92:255509, 2004.

Y.G. Lei, C.M. Chan, Y. Wang, K.M. Ng, Y. Jiang, and L. Lin. *Polymer*, 44:4673, 2003.

J.K. Hobbs. *Chinese J. Polym. Sci.*, 21:135, 2003.

P. Kohn. *Diplomarbeit*. Physikalisches Institut, Universität Freiburg, 2004.

A. Häfele, B. Heck, T. Kawai, P. Kohn, and G. Strobl. *Eur. Phys. J.-E*, 16:207, 2005.

G. Hauser, J. Schmidtke, and G. Strobl. *Macromolecules*, 31:6250, 1998.

B. Heck, S. Siegenführ, and G. Strobl. *Polymer*, in press, 2007.

B. Heck, T. Hugel, M. Iijima, E. Sadiku, and G. Strobl. *New J. Physics*, 1:17.1, 1999.

C. Fougnies, M. Dosiére, M.H.J. Koch, and J. Roovers. *Macromolecules*, 18:6266, 1998.

T. Hippler, S. Jiang, and G. Strobl. *Macromolecules*, 38:9396, 2005.

T.Y. Cho, W. Stille, and G. Strobl. *Colloid Polym. Sci.*, in press, 2007.

G.R. Strobl, T. Engelke, H. Meier, and G. Urban. *Colloid Polym. Sci.*, 260:394, 1982.

G.R. Strobl, M.J. Schneider, and I.G. Voigt-Martin. *J. Polym. Sci.*, 18:1361, 1980.

K. Schmidt-Rohr and H.W. Spieß. *Macromolecules*, 24:5288, 1991.